DMD Fast Forward. Published on March 5, 2008 as doi:10.1124/dmd.107.020321

PDZK1 REGULATES TWO INTESTINAL SOLUTE CARRIERS (Slc15a1 and Slc22a5) IN MICE

TOMOKO SUGIURA, YUKIO KATO, TOMOHIKO WAKAYAMA, DAVID L. SILVER, YOSHIYUKI KUBO, SHOICHI ISEKI, AKIRA TSUJI

Division of Pharmaceutical Sciences, Graduate School of Natural Science and Technology (T.S., Y.K., Y.K., A.T.) and Department of Histology and Embryology, Graduate School of Medical Science (T.W., S.I.), Kanazawa University, Kanazawa, Ishikawa 920-1192, Japan, and Department of Biochemistry, Albert Einstein College of Medicine (D.L.S.), 1300 Morris Park Ave, Bronx, NY 10461, USA

Running title:

PDZK1 regulates PEPT1 and OCTN2 in mouse small intestine

Corresponding author :

Prof. Akira Tsuji, Ph.D

Division of Pharmaceutical Sciences, Graduate School of Natural Science and Technology, Kanazawa University, Kakuma, Kanazawa 920-1192, Japan

Tel:(81)-76-234-4479/Fax:(81)-76-264-6284/

Email: tsuji@kenroku.kanazawa-u.ac.jp

Document statistics:

number of text pages: 37

number of table: 0

number of figures: 8

number of references: 39

number of words:

Abstract: 247

Introduction: 774

Discussion: 1562

Abbreviations: PEPT1, oligopeptide transporter 1; OCTN2, carnitine/organic cation transporter 2; SLC, solute carrier; PDZ, postsynaptic density 95/disk-large/ZO-1; HEK, human embryonic kidney; BBMV, brush-border membrane vesicle; PBS, phosphate-buffered saline; YFP, yellow fluorescent protein

DMD Fast Forward. Published on March 5, 2008 as DOI: 10.1124/dmd.107.020321
This article has not been copyedited and formatted. The final version may differ from this version.

ABSTRACT

Gastrointestinal absorption of certain therapeutic agents is thought to be mediated by solute carrier (SLC) transporters, though minimal *in vivo* evidence has been reported. Here, we demonstrate key roles of PDZ domain-containing protein, PDZK1, as a regulatory mechanism of two solute carriers, Slc15a1 (oligopeptide transporter PEPT1) and Slc22a5 (carnitine/organic cation transporter OCTN2) in mouse small intestine by using *pdzk1* gene knockout (*pdzk1*$^{-/-}$) mice. Gastrointestinal absorption of cephalexin, a substrate of PEPT1, after oral administration was delayed in *pdzk1*$^{-/-}$ mice compared with wild-type mice. Absorption of carnitine, a substrate of OCTN2 was also decreased in *pdzk1*$^{-/-}$ mice. Immunohistochemical analysis revealed the localization of both PEPT1 and OCTN2 at apical membrane of small intestinal epithelial cells in wild-type mice, whereas such apical localization was reduced in *pdzk1*$^{-/-}$ mice, with a concomitant decrease in their protein levels assessed by Western blotting in intestinal brush-border membranes. Electron microscopy revealed localization of PEPT1 in intracellular vesicular structures in *pdzk1*$^{-/-}$ mice. In addition, we first identified interaction between PEPT1 and PDZK1 in mouse small intestine, and found that PDZK1 stimulates transport activity of PEPT1 by increasing its expression level in HEK293 cells. Taken together, the present findings provide direct evidence that PDZK1 regulates two intestinal SLC transporters *in vivo* as an adaptor protein for these transporters, and affects oral absorption of their substrates. These findings also raise the possibility that intestinal absorption of the substrate drugs for PEPT1 and OCTN2 is governed by protein network of these transporters and their adaptor PDZK1.

INTRODUCTION

The membrane of intestinal epithelial cells is the first barrier to the absorption of therapeutic agents into the circulation, and permeation across this membrane is one of the critical factors determining oral bioavailability. It had been considered that intestinal absorption of lipophilic drugs is governed by simple diffusion according to the pH-partition hypothesis, but the intestinal absorption of several hydrophilic drugs, including amino ß-lactam antibiotics, could not be simply explained by passive diffusion (Tsuji et al., 1979), and therefore carrier-mediated system(s) were suggested to be involved in the intestinal absorption (Tsuji et al., 1981). Since then, many studies have established the involvement of oligopeptide-specific transporters in the absorption of certain types of ß-lactam antibiotics (Tsuji and Tamai, 1996).

The H^+/oligopeptide transporter PEPT1 (SLC15A1) is localized on apical membranes of small intestinal epithelial cells and recognizes not only di- and tripeptides, but also peptide-like drugs, including oral ß-lactam antibiotics, angiotensin-converting enzyme inhibitor, rennin inhibitor and bestatin (Hu and Amidon, 1988; Frieman and Amidon, 1990; Kramer et al., 1990; Saito et al., 1993; Tamai et al., 1997; Nakanishi et al., 1997). Moreover, intestinal uptake and permeability of some ß-lactam antibiotics is well correlated with the expression level of PEPT1 in the small intestine (Chu et al., 2001; Naruhashi et al., 2002). These data suggest that at least certain types of ß-lactam antibiotics might be absorbed mainly via PEPT1 in the small intestine.

Transport of substrates by PEPT1 is known to be electrogenic, utilizing the proton gradient across the plasma membrane as a driving force (Ganapathy and Leibach, 1985). This proton gradient is produced by another transporter, Na^+/H^+ exchanger (NHE), which pumps out protons utilizing the Na^+ gradient as a driving force. Thus,

NHE is thought not only to supply the driving force for PEPT1, but also to export protons transported by PEPT1 together with its substrates to maintain the proton balance across the plasma membrane. Thus, it is hypothesized that transport function of PEPT1 is also affected by NHE activity. This idea has been supported by the observation in gastrointestinal epithelial cells, Caco-2, and HEK293 cells transiently transfected PEPT1 and NHE3 (Kennedy et al., 2002; Thwaites et al., 2002; Watanabe et al., 2005). It is thus possible that NHE is localized in proximity to PEPT1 to maintain its transport function, and such cooperation with other transporter(s) may be a key feature of PEPT1 function. However, little information is available on protein-protein interactions involving PEPT1 in the small intestine.

On the other hand, carnitine/organic cation transporter OCTN2 (SLC22A5) is also localized on apical membrane of small intestinal and renal epithelial cells, and is physiologically important for intestinal absorption and renal tubular reabsorption of its endogenous substrate, carnitine, which plays an important role for the ß-oxidation of fatty acids in mitochondria (Nezu et al 1999; Kato et al., 2006). Recently we have revealed that OCTN2 colocalized with PDZ (PSD-95/Dlg/ZO-1) domain-containing protein PDZK1 on apical membrane of absorptive epithelial cells, and OCTN2 interacts with PDZK1 in mouse small intestine (Kato et al., 2006). PDZK1 has four PDZ domains in its structure, and each PDZ domain alone can directly bind to C-terminus of various transporters. PDZK1 has been suggested to be a functional regulator of various transporters and may be a scaffold protein that links those transporters at certain microdomains on epithelial cell-surface (Gisler et al., 2003; Kato et al., 2004, 2005; Sugiura et al., 2006; Anzai et al., 2004; Miyazaki et al., 2005), raising the possibility that PDZK1 interacts with various intestinal transporters including OCTN2 and PEPT1.

However, most of the data suggesting such functional regulation by PDZK1 were obtained in *in vitro* double transfection studies with cultured cell lines. Although Wang et al. (2005) recently demonstrated an essential role of PDZK1 in basolateral expression of organic anion transporting peptide 1a1 in the liver, the *in vivo* evidence for a fundamental role of PDZK1 as a regulatory mechanism for xenobiotic transporters is quite limited in small intestine.

In the present study, we focused on PDZK1 as a candidate regulator of PEPT1 and OCTN2, and examined its pharmacological relevance *in vivo*. A pharmacokinetic study of cephalexin (a substrate of PEPT1) and carnitine (a substrate of OCTN2) using *pdzk1* gene knockout mice (*pdzk1*$^{-/-}$) was performed to clarify the role of PDZK1 in intestinal absorption of substrates of intestinal transporters. In addition, *in vitro* studies were also performed to support the regulatory role of PDZK1 for PEPT1. Our findings show that both PEPT1 and OCTN2 are regulated *in vivo* by an interaction with PDZK1 in the small intestine. The present findings also provided further support for a fundamental role of PEPT1 in the intestinal absorption of ß-lactam antibiotics *in vivo*.

DMD Fast Forward. Published on March 5, 2008 as DOI: 10.1124/dmd.107.020321
This article has not been copyedited and formatted. The final version may differ from this version.

MATERIALS AND METHODS

Materials

Rabbit polyclonal antibody to PEPT1, rabbit polyclonal antibody to OCTN2 and rat polyclonal antibody to PDZK1 were raised as described previously (Sai et al., 1996; Tamai et al., 2000; Kato et al., 2005). Monoclonal antibodies against c-myc epitope tag (9E10), green fluorescent protein (GFP), glyceraldehyde 3 phosphate dehydrogenase (GAPDH) and ß-actin (AC-15) were obtained from Covance Inc. (Princeton, NJ), Roche Diagnostics (Basel, Switzerland), Chemicon International, Inc. (Temecula, CA) and Sigma-Aldrich, Inc. (St. Louis, MO), respectively. [^{3}H]Glycylsarcosine (GlySar, 0.5 Ci/mmol) and [^{14}C]mannitol (53 mCi/mmol) were purchased from Moravek Biochemicals Inc. (Mercury Lane, Brea, CA), and L-[^{3}H]carnitine (84 Ci/mmol) was purchased from GE Healthcare (Piscataway, NJ), and [^{14}C]inulin (1-3 mCi/g) was purchased from PerkinElmer Life Sciences (Boston, MA). Cephalexin hydrate was purchased from Sigma-Aldrich Japan K.K. (Tokyo, Japan). Antipyrine was provided from Wako Pure Chemical Industries (Osaka, Japan). The protein assay kit was purchased from Bio-Rad Laboratories, Inc. (Hercules, CA). cDNA encoding full-length human PEPT1 was subcloned into the pEYFP-C1 vector (Clontech). Other reagents were obtained from Sigma Chemical Co. (St. Louis, MO), Wako Pure Chemical Industries (Osaka, Japan), Funakoshi Co. (Tokyo, Japan) and Nacalai Tesque, Inc. (Kyoto, Japan), and used without further purification.

Animals

Male mice were used for all experiments at 6 – 12 weeks of age. *pdzk1*$^{-/-}$ mice had been previously produced (Lan and Silver, 2005). *pdzk1*$^{-/-}$ and littermates were of a

mixed genetic background (C57BL/6J and 129Sv/Ev) produced by intercrossing *pdzk1*$^{+/-}$ mice. They had free access to food and water. This study was carried out in accordance with the Guide for the Care and Use of Laboratory Animals in Takara-machi Campus of Kanazawa University.

Pharmacokinetic Studies

Mice were fasted overnight with free access to water and anesthetized with diethylether during drug administration and blood sampling. Cephalexin (2.0 mg/kg body weight), [^{3}H]carnitine (250 ng/kg body weight) and antipyrine (20 mg/kg body weight) were orally administered by gavage. At various intervals after administration, aliquots of blood samples were collected through the caudal vein. All blood samples were immediately centrifuged to obtain plasma, which was further mixed with two volumes of acetonitrile, then centrifuged, and the resultant supernatant was used for quantitation.

The Amount of [^{3}H]Carnitine Retaining in GI Tract after Oral Administration

[^{3}H]Carnitine and [^{14}C]inulin were dissolved in saline and orally administered by gavage. The initial concentration of carnitine was 125 ng/mL and the volume of the solution administered was 2 mL/kg. Then, mice were sacrificed at 30 min after administration and their abdomen was opened immediately to take the sample of residual [^{3}H]carnitine and [^{14}C]inulin from each segment of the GI tract. The mouse alimentary tract was divided as follows: stomach, upper small intestine, middle small intestine, lower small intestine, cecum and large intestine.

Uptake Studies in Everted Intestinal Sac

An everted intestinal sac was prepared from the upper, middle and lower part of the small intestine of wild-type and *pdzk1*$^{-/-}$ mice. After 5 min of preincubation in the transport buffer (125 mM NaCl, 4.8 mM KCl, 1.2 mM KH_2PO_4, 5.6 mM D-glucose, 1.2 mM $CaCl_2$, 1.2 mM $MgSO_4$ and 25 mM MES; pH 6.0). the sac was incubated with [^{3}H]carnitine and [^{14}C]mannitol (extracellular marker) at 37˚C for the designated times. The sac was then washed with ice-cold buffer, weighed and solubilized in Soluene-350 Packard Co., Canberra, Australia) by incubation at room temperature for 24 hr. The solubilized samples were decolorized with 0.2 mL of H_2O_2, neutralized with 0.1 mL of 5 N HCl, left at room temperature for 4 hr and mixed with 3 mL of a scintillation cocktail. Radioactivity was then counted using a liquid scintillation counter.

Analytical Procedures

Cephalexin and antipyrine were measured with a LC/MS/MS system equipped with a constant flow pump (Agilent 1200 series G1312A, Agilent Technologies, Tokyo, Japan), an automatic sample injector (G1367B; Agilent Technologies), a column oven (G1316A; Agilent Technologies) and a mass spectrometer (API 3200, Applied Biosystems, Tokyo, Japan). For cephalexin, the analytical column was COSMOSIL® AR-II (2.0 mm x 150 mm; Nacalai Tesque, Kyoto, Japan). Mobile phase A was 0.01 M ammonium formate and mobile phase B was 100% methanol. The gradient elution time program was set as follows: 0-4 min, B 5-35%; 4-16 min, B 35%; 16.1-25 min, B 5%. The flow rate was 0.2 mL/min. For antipyrine, the column was COSMOSIL® MS-II (2.0 mm x 50 mm; Nacalai Tesque, Kyoto, Japan), and the gradient elution time program was set as follows: 0-1 min, B 7-70%; 1-9.5 min, B 70%; 9.6—19.6 min, B 7%.

The radioacvitity of [^{3}H]GlySar, [^{3}H]carnitine and [^{14}C]mannitol were measured with a liquid scintillation counter, LSC-5100 (Aloka, Japan) with Clearsol I (Nacalai Tesque, Inc.) as a scintillation fluid.

Immunohistochemical Analysis

Frozen sections of mouse small intestine were prepared as described previously (Kato et al., 2006). Following successive pretreatments with 0.3% Tween 20 in PBS, 0.3% H_2O_2 in methanol and 5% BSA in PBS, the sections were incubated with anti-PEPT1 or anti-OCTN2 antibody. They were washed with PBS, and the immunoreaction product was visualized by incubating the section successively with biotinylated anti-rabbit IgG (Vector Laboratories, Burlingame, CA) for 2 h, horseradish peroxidase-conjugated streptavidin (DakoCytomation, Kyoto, Japan) for 1 h and 3',3'-diaminobenzidine tetrahydrochloride (DAB) containing H_2O_2 for a few minutes. Finally, they were mounted in Vectashield mounting medium with DAPI (Vector Laboratories) to fix the sample. The specimens were examined with an Axiovert S 100 microscope (Carl Zeiss, Jena, Germany).

For electron microscopic immunocytochemistry, the pre-embedding immunoreaction method was employed (Wakayama et al. 2004). Cryosections immunostained with anti-PEPT1 antibody were postfixed in 0.5% OsO_4 for 20 min, stained with 1% uranyl acetate for 20 min, dehydrated in a graded ethanol series and embedded in Glicidether 100 (Selva Fenbiochemica, Heidelberg, Germany). Ultrathin sections were cut with an ultramicrotome and observed with a JEM-1210 electron microscope (JEOL, Tokyo, Japan).

Immunoprecipitation and Western Blot Analysis of Intestinal Brush-Border Membrane Vesicles (BBMVs)

BBMVs were prepared from mouse small intestine as described by Tsuji et al. (1987) with some modifications. Briefly, the mucosa was scraped off and homogenized in ice-cold 2 mM Tris-HCl buffer (pH 7.1) containing 50 mM mannitol, in a volume (milliliters) equal to 30 times the weight (grams) of the mucosa scrapings. Homogenization was carried out with a ULTRA-TURRAX T25 for 5 min at the maximum speed. $CaCl_2$ solution (1 M) was added to the homogenate to give a final concentration of 10 mM, and the mixture was stirred in a cold room for 15 min. It was then centrifuged at 3,000 x g for 15 min, and the supernatant was centrifuged at 27,000 x g for 30 min. The resultant pellet was resuspended in a washing medium, through a 25-gauge needle. The washing medium used was 10 mM Tris-HEPES buffer (pH 7.5) containing 270 mM mannitol.

Intestinal BBMVs thus obtained were solubilized in RIPA-Y buffer containing 1% Nonidet P-40, 75 mM NaCl, 50 mM Tris-HCl, pH 7.5 and protease inhibitors. Anti-PDZK1 antibody prebound to Protein L Sepharose (Pierce Chemical, Rockford, IL) or anti-PEPT1 antibody prebound to Protein G Sepharose (Amersham) was added to the obtained lysate, and the mixture was incubated at 4 ˚C for 8 hr, followed by centrifugation and washing three times with phosphate-buffered saline. Samples were analyzed by SDS-polyacrylamide gel electrophoresis, followed by immunoblotting with anti-PEPT1 or anti-OCTN2 antibody. Western blot analysis was performed as described previously (Kato et al., 2005).

Determination of mRNA Expression by Real-time PCR

Total RNAs were extracted from small intestine of wild-type and *pdzk1*$^{-/-}$ mice (male, 8 weeks), and cDNA was synthesized as described previously (Naruhashi et al., 2002). Quantification of the mRNA coding PEPT1 and ß-actin was performed using LightCycler® technology (Roche Diagnostics). The PEPT1 forward and reverse primers were 5'-AGGGTCACCGGCACAACCTT-3' and 5'-GACGGAGCCTGGGAATAAGAG-3', respectively, which produce a 469 bp amplicon. The ß-actin forward and reverse primers were 5'-AGAGGGAAATCGTGCGTGACA-3' and 5'-CAATAGTGATGACCTGGCCGT-3', respectively, which produce a 138 bp amplicon. The PCR conditions for PEPT1 were as follows: initial denaturation at 95˚C for 10 min, followed by 45 cycles of denaturation at 95 ºC for 0 seconds (followed by an immediate change to the next temperature) and combined annealing-extension at 60 ºC for 0 seconds and 72 ºC for 19 seconds, followed by fluorescence emission reading at 78 ºC for 10 seconds. In the case of the PCR for ß-actin, the annealing temperature was 58 ˚C for 0 sec, and the extension temperature was 72˚C for 6 sec. The quantification value was calculated as the average of three determinations of each of three different dilutions.

Transport Studies in Cell Culture

HEK293 cells were routinely grown in Dulbecco's modified Eagle's medium containing 10% fetal calf serum, penicillin, and streptomycin in a humidified incubator at 37˚C and 5% CO_2. HEK293 cells stably expressing myc-tagged PDZK1 (HEK293/PDZK1 cells) were previously obtained (Kato et al., 2004), and were grown under the same conditions, except that the medium also contained 0.1% G-418. cDNA encoding human PEPT1 was subcloned into the pEYFP-C1 vector (BD Biosciences

DMD Fast Forward. Published on March 5, 2008 as DOI: 10.1124/dmd.107.020321
This article has not been copyedited and formatted. The final version may differ from this version.

Clontech). cDNA encoding PEPT1Δ4 (with deletion of the last four amino acids) was amplified from pEYFP-C1/PEPT1 by PCR using 5'- and 3'-specific primers (5'-AGATCTGCCGCCATGGGAATGTCCAAATC-3' and 5'-CAATTCACAGAAACAGATGTGAGTCGAC-3', respectively). The PCR product was subcloned into the pEYFP-C1 vector using *Bgl* II/*Sal* I sites, and sequence for the insert was verified. After 24 hr cultivation, the cDNA construct was transiently transfected into HEK293 or HEK293/PDZK1 cells by adding 20 μg/15 cm dish of the plasmid DNA according to the calcium phosphate precipitation method (Tamai et al., 2000). At 48 hr after transfection, cells were harvested and suspended in transport medium (125 mM NaCl, 4.8 mM KCl, 5.6 mM D-glucose, 1.2 mM $CaCl_2$, 1.2 mM KH_2PO_4, 1.2 mM $MgSO_4$, and 25 mM HEPES, pH 7.4). A [^{3}H]GlySar uptake experiment was then performed according to the silicone-oil layer method (Tamai et al., 2000). According to our preliminary analysis, uptake of [^{3}H]GlySar was linear until 3 min, and therefore, initial uptake was examined at 3 min as reported previously (Watanabe et al., 2005). To analyze transport of cephalexin, the cell suspension and the transport medium containing cephalexin (100 μM) were mixed to initiate the transport reaction. At the designated times, 200 μL aliquots of the mixture were withdrawn, and the cells were separated from the transport medium by centrifugal filtration through a layer of a mixture of silicon oil (SH550; Toray Dow Corning, Tokyo, Japan) and liquid paraffin (Wako Pure Chemicals, Osaka, Japan) on top of 3 M KCl solution. After sonication, cells was deproteinized with acetonitrile, then centrifuged for 5 min at 15,000 g, and the resulting supernatant was measured by LC/MS/MS.

Subcellular Localization and Immunoprecipitation Analysis in HEK293 Cells

DMD Fast Forward. Published on March 5, 2008 as DOI: 10.1124/dmd.107.020321
This article has not been copyedited and formatted. The final version may differ from this version.

HEK293 cells were grown on cover glass (15 × 15 mm; thickness, 0.12-0.17 mm; Matsunami Glass Inc., Osaka, Japan) and transiently transfected with cDNA encoding YFP-PEPT1. At 48 hr after the transfection, cells were fixed with 3% formaldehyde in phosphate-buffered saline (PBS). Attached cells were sealed onto the slides using Vectrashield mounting medium with 4',6-dianidino-2-phenylindole (Vector Laboratories, Burlingame, CA), and the fluorescence was detected with a confocal laser scanning fluorescence microscope (LSM 510; Carl Zeiss, Jena, Germany). At 48 hr after transfection of YFP-PEPT1 in HEK293/PDZK1, the cells were washed twice with PBS, harvested and solubilized in RIPA-Y buffer. Western blot analysis was then performed using anti-GFP or anti-GAPDH antibodies as described previously (Kato et al., 2005). For immunoprecipitation, cell lysate was added to anti-myc antibody prebound to Protein L Sepharose (Pierce Chemical, Rockford, IL), and the mixture was incubated at 4˚C for 8 hr, followed by centrifugation, washing three times with PBS, and Western blot analysis.

Data Analysis

The results are expressed as mean ± S.E.M. and statistical analysis was performed by using Student's *t*-test. A difference between means was considered to be significant when $p < 0.05$. Fitting of plasma concentration-time profiles based on compartmental analysis was performed using the MULTI program.

DMD Fast Forward. Published on March 5, 2008 as DOI: 10.1124/dmd.107.020321
This article has not been copyedited and formatted. The final version may differ from this version.

RESULTS

Characterization of the Interaction of PEPT1 and PDZK1 in HEK 293 cells

Coexpression with PDZK1 increased the apparent uptakes by several SLC transporters of their substrates in HEK293 cells, although the effect of PDZK1 on PEPT1 has not yet been examined. To examine whether the function of PEPT1 is modulated by PDZK1, uptake study was first performed in HEK293/PDZK1 cells transiently expressing PEPT1 in the present study. Time-dependent uptake of [^{3}H]GlySar by PEPT1 was observed in both HEK293 and HEK293/PDZK1 cells, with the initial slope of the uptake being higher in HEK293/PDZK1 cells than in HEK293 cells (Fig. 1A). To examine the structural requirements at the C-terminus of PETP1 for the regulation of PEPT1, a mutant construct, PEPT1Δ4, lacking the last four amino acids of PEPT1 (-QKQM) was constructed. [^{3}H]GlySar uptake by PEPT1Δ4 was also higher in HEK293/PDZK1 than HEK293 cells (Fig. 1D). As in the case of [^{3}H]GlySar uptake, uptake of cephalexin mediated by PEPT1 was stimulated in the presence of PDZK1 (Fig. 1C). Saturable uptake of GlySar was observed during transient expression of PEPT1 in both HEK293/PDZK1 and HEK293 cells. Eadie-Hofstee plots revealed the existence of a single component, with a similar slope for the two cell lines, for the saturable uptake. The obtained values for K_m and V_{max} were 0.516 ± 0.015 and 0.549 ± 0.128 mM, and 2.74 ± 0.12 and 5.61 ± 1.26 nmol/mg protein/3 min in HEK293 and HEK293/PDZK1 cells, respectively (Fig. 1B).

To examine the physical interaction of PEPT1 and PDZK1 in HEK293 cells, we next performed immunoprecipitation using anti-myc antibody (to myc-PDZK1) in lysates of HEK293/PDZK1 cells transiently transfected with PEPT1, followed by Western blot analysis using anti-GFP antibody, since HEK293/PDZK1 cells stably

express myc-tagged PDZK1, while PEPT1 was transiently transfected as a YFP fusion protein. Immunoprecipitation with c-myc antibody resulted in a predicted band of approximately 100 kDa with immunoreactivity to GFP antibody (Fig. 2A, *left panel, lane 3*). This YFP-PEPT1 band was also observed when PEPT1Δ4 was transfected (Fig. 2A, *left panel, lane 4*), but not when PDZK1 was not stably expressed or when PEPT1 was not transiently transfected (*lanes 1 and 2*, respectively). Immunoprecipitation also yielded a 75 kDa protein that was immunoreactive with c-myc antibody (Fig. 2A, *right panel*) having the predicted molecular weight for myc-PDZK1.

The subcellular localization of PEPT1 and its possible colocalization with PDZK1 were further examined. In both HEK293 and HEK293/PDZK1 cells, PEPT1 was mainly localized in plasma membranes with some minor localization in intracellular space (Fig. 2C). To compare expression levels of PEPT1, Western blot analysis was then performed for cellular lysates from HEK293 or HEK293/PDZK1 transiently transfected with PEPT1. Expression of PEPT1 was slightly higher in HEK293/PDZK1 cells compared with HEK293 cells (Fig. 2B, *upper panel*). Expression of endogenous GAPDH, examined in a control experiment, was comparable in the two lines (Fig. 2B, *lower panel*). The fold increase in the PEPT1 expression was 1.7 when normalized to GAPDH expression, and this value approximated the difference in the uptake of [^{3}H]GlySar (Fig. 1A).

Physical Interaction between PEPT1 and PDZK1 in Mouse Small Intestine

To examine the possible interaction between PDZK1 and PEPT1 under physiological conditions, immunoprecipitation of lysates of intestinal BBMVs was performed using anti-PDZK1 antibody, followed by Western blot analysis with anti-

DMD Fast Forward. Published on March 5, 2008 as DOI: 10.1124/dmd.107.020321
This article has not been copyedited and formatted. The final version may differ from this version.

PEPT1 antibody (Fig. 3A). PEPT1 was detected in anti-PDZK1 immunoprecipitates together with PDZK1, but not when preimmune control serum was used for immunoprecipitation (Fig. 3A). These results revealed that PEPT1 interacts with PDZK1 in mouse small intestine, as in case between OCTN2 and PDZK1 (Kato et al., 2006).

Reduced Expression of PEPT1 and OCTN2 on the Apical Membranes of the Small Intestine in *pdzk1*$^{-/-}$ Mice

To further examine the interaction of PDZK1 with PEPT1 and OCTN2, *pdzk1*$^{-/-}$ mice were used to analyze the change in expression and localization of these transporters in the small intestine of *pdzk1*$^{-/-}$ mice. Immunoreactive bands of PEPT1 and OCTN2 assessed in Western blot analysis were found to be expressed in the small intestine from wild-type mice, while these transporters in the small intestine from *pdzk1*$^{-/-}$ mice were less than wild-type mice (Fig. 3B). We confirmed by Western blot analysis that PDZK1 protein was not expressed in *pdzk1*$^{-/-}$ mice, in contrast with wild-type mice (Fig. 3B). Expression of ß-actin was observed in all samples of small intestine (Fig. 3B).

We also undertook an immunohistochemistry analysis of PEPT1 and OCTN2 in the small intestine from wild-type and *pdzk1*$^{-/-}$ mice (Fig. 4). PEPT1 and OCTN2 were localized on the apical brush-border membrane in wild-type mice (Fig. 4A, 4C). However, in *pdzk1*$^{-/-}$ mice, PEPT1 and OCTN2 stainings at the apical surface were noticeably weaker in the small intestine (Fig. 4B, 4D). These results were compatible with the results of Western blot analysis (Fig. 3B).

DMD Fast Forward. Published on March 5, 2008 as DOI: 10.1124/dmd.107.020321
This article has not been copyedited and formatted. The final version may differ from this version.

We also examined the mRNA copy number of PEPT1 in the upper intestine from both wild-type and *pdzk1*$^{-/-}$ mice by real-time quantitative PCR analysis. PEPT1 mRNA expression normalized to that of ß-actin was not significantly different in *pdzk1*$^{-/-}$ compared to wild-type mice (Fig. 3C), indicating that changes in PEPT1 levels occurred on a post-transcriptional level.

Subcellular Localization of PEPT1 in Absorptive Epithelial Cells

The subcellular localization of PEPT1 in mouse small intestine was further analyzed by immunoelectron microscopy (Fig. 5A, 5B). Immunoreactivity of PEPT1 in wild-type mice was mainly found in microvilli in the apical region of absorptive epithelial cells (Fig. 5A). However, in *pdzk1*$^{-/-}$ mice, immunoreactivity of PEPT1 on microvilli was quite weak, but slight, diffuse immunoreactivity was seen in the cytoplasmic region of the absorptive epithelial cells (Fig. 5B). In wild-type mice, the localization of PEPT1 was similar to that of the terminal web of actin filaments, as in the cases of OCTN2 and PDZK1 (Kato et al., 2006). The ultrastructural abnormality of the intestinal epithelial cells was observed in *pdzk1*$^{-/-}$ mice (Fig. 5D). In *pdzk1*$^{-/-}$ mice, vesicular structures were more obviously found in the cytoplasm of absorptive epithelial cells, compared with wild-type mice (Fig. 5C, 5D).

Intestinal Absorption of Cephalexin, Carnitine and Antipyrine in Wild-type and *pdzk1*$^{-/-}$ Mice

To investigate the role of PDZK1 in intestinal drug absorption *in vivo*, a mixture of several ß-lactam antibiotics (cephalexin, cephradine, cefaclor, cefatridine) was intravenously or orally administered to both wild-type and *pdzk1*$^{-/-}$ mice, followed

by LC/MS/MS measurement of the plasma concentration-time profile of each compound. Plasma concentrations of the intravenously infected compounds exhibited only minimal differences between wild-type and *pdzk1*$^{-/-}$ mice, whereas those after oral administration exhibited slight, but consistent differences between the two strains for all four compounds examined (data not shown). Based on these initial findings, we next investigated in detail the pharmacokinetic profile of cephalexin, a known substrate of PEPT1. Intravenous administration of cephalexin resulted in similar monophasic plasma concentration-time profiles in wild-mice and *pdzk1*$^{-/-}$ mice (data not shown). In contrast, plasma concentration of cephalexin after oral administration was lower in *pdzk1*$^{-/-}$ mice than that in wild-type mice (Fig. 6A). Since gastrointestinal absorption of cephalexin is thought to be mediated by PEPT1 expressed on the apical membrane of the small intestine, it is possible that the delay of cephalexin absorption in *pdzk1*$^{-/-}$ mice (Fig. 6A) is caused by a defect of PEPT1 in plasma membrane (Fig. 4, 5).

Plasma concentration of radioactivity after oral administration of [^{3}H]carnitine, a substrate of OCTN2, was lower in *pdzk1*$^{-/-}$ mice compared with wild-type mice (Fig. 6B). Our previous report suggested that OCTN2 plays a predominant role for the uptake of carnitine from apical surface of mouse small intestine (Kato et al., 2006). Decreased absorption of carnitine (Fig. 6B) was presumably caused by decreased the expression of OCTN2 at apical membrane of intestinal epithelial cells in *pdzk1*$^{-/-}$ mice (Fig. 4). In contrast, the plasma concentration of antipyrine after oral administration was similar between wild-type and *pdzk1*$^{-/-}$ mice (Fig. 6C).

Since L-carnitine is known to be converted to acetylcarnitine and other acylcarnitines in tissues (Rebouche and Paulson 1986), we measured the amount of [^{3}H]carnitine retained in GI tract at 30 min after oral administration (Fig. 7A). An

DMD Fast Forward. Published on March 5, 2008 as DOI: 10.1124/dmd.107.020321
This article has not been copyedited and formatted. The final version may differ from this version.

extracellular marker [^{14}C]inulin retained in GI tract was also measured (Fig. 7B). [^{14}C]Inulin retained in each segment of GI tract was similar, and total recovery of [^{14}C]inulin was approximately 100% in both wild-type and *pdzk1*$^{-/-}$ mice (Fig. 7B). On the other hand, [^{3}H]carnitine retained in upper and middle parts of small intestine was higher in *pdzk1*$^{-/-}$ mice than that in wild-type mice (Fig. 7A), indicating that absorption of [^{3}H]carnitine was smaller in *pdzk1*$^{-/-}$ mice compared with wild-type mice. Moreover, the uptake of carnitine from the apical surface into the everted intestinal tissue was investigated (Fig. 8). The uptake of [^{3}H]carnitine from apical surface by the intestinal tissue was much higher in wild-type mice than that in *pdzk1*$^{-/-}$ mice, and decreased in the presence of 20 mM unlabeled carnitine (Fig. 8). The extracellular space assessed as the apparent uptake of [^{14}C]mannitol was almost similar between wild-type and *pdzk1*$^{-/-}$ mice (0.11 ± 0.01 and 0.14 ± 0.02 μL/mg tissue, respectively).

DISCUSSION

The H^+/oligopeptide transporter PEPT1 (SLC15A1) is thought to be involved in absorption of di- and tripeptides, as well as various types of therapeutic agents, including ß-lactam antibiotics. In a previous report, we showed that intestinal transport of another ß-lactam antibiotic, cefadroxil, is correlated with the PEPT1 expression level in the small intestine of both fed and starved rats (Naruhashi et al., 2002). Thus, at least some ß-lactam antibiotics might be absorbed mainly via PEPT1 in the small intestine. Despite the transport activity of PEPT1, the regulatory mechanisms of this transporter *in vivo* are still poorly understood. Our findings here indicate that PEPT1 is functionally regulated by PDZK1 in mouse small intestine, and is likely to be involved in gastrointestinal absorption of cephalexin *in vivo*. The following four lines of evidence support this conclusion: First, after oral administration of cephalexin *in vivo*, plasma concentration was lower in *pdzk1*$^{-/-}$ mice, compared with wild-type mice (Fig. 6A), suggesting intestinal absorption of cephalexin was decreased in *pdzk1*$^{-/-}$ mice. Second, in *pdzk1*$^{-/-}$ mice PEPT1 levels on apical membranes of small intestine were reduced compared with wild-type mice (Fig. 4, 5), with a concomitant decrease in its protein expression level in BBMVs of the small intestine (Fig. 3B). Third, PEPT1 is immunoprecipitated by antibody to PDZK1 (Fig. 3A), suggesting a physical interaction of the two proteins, that was confirmed *in vitro* in HEK293 cells transfected with these proteins (Fig. 2A). Fourth, coexpression with PDZK1 affected the PEPT1 expression level in HEK293 cells (Fig. 2B), thereby increasing PEPT1-mediated transport of substrates, GlySar and cephalexin (Fig. 1A, 1C), with an increase in transport capacity (Vmax, Fig. 1D). This *in vitro* result seems consistent with the reduction of PEPT1 on the apical membrane of *pdzk1*$^{-/-}$ mice *in vivo* (Fig. 4, 5). Together, these data indicate

that PDZK1 is a regulatory factor of PEPT1 levels and function in mouse small intestine, providing the first demonstration of the potential pharmacological role of PEPT1-PDZK1 complex in small intestine *in vivo*.

Similarly, plasma concentration of [^{3}H]carnitine after oral administration was decreased in *pdzk1*$^{-/-}$ mice compared with wild-type mice (Fig. 6B), suggesting intestinal absorption of carnitine was decreased in *pdzk1*$^{-/-}$ mice, as in case of juvenile visceral steatosis (*jvs*) mice, which have a hereditary deficiency of the *octn2* gene (Yokogawa et al., 1999; Kato et al., 2006). The reduced oral absorption of carnitine in *pdzk1*$^{-/-}$ mice was also supported by the elevated [^{3}H]carnitine retained in the GI tract after oral administration (Fig. 7) and decreased uptake by the intestinal tissue from apical surface (Fig. 8) in *pdzk1*$^{-/-}$ mice. We have recently reported that OCTN2 is localized with PDZK1 in microvilli of absorptive epithelial cells, and uptake of carnitine was quite small and unsaturable in enterocytes obtained from *jvs* mice (Kato et al., 2006), suggesting carnitine is mainly transported by intestinal OCTN2. In *pdzk1*$^{-/-}$ mice, reduced expression of intestinal OCTN2 (Fig. 4C, 4D) might lead to the decreased intestinal absorption of carnitine. On the other hand, plasma concentration of antipyrine, a marker compound for passive diffusion, was similar between wild-type and *pdzk1*$^{-/-}$ mice (Fig. 6C), suggesting that PDZK1 may affect only the substrates of intestinal transporters which interact with PDZK1 in the small intestine. From in vitro investigation, OCTN2 could recognize other organic cation drugs including verapamil and quinidine (Ohashi et al., 2001), thereby OCTN2 could be a possible target for oral delivery of therapeutic agents.

Although the transport activity of oligopeptide and carnitine was reduced in small intestine of *pdzk1*$^{-/-}$ mice, no obvious phenotypic change except hyperlipemia has

been reported in *pdzk1*$^{-/-}$ mice (Kocher et al., 2003, Lan and Silver, 2005). In *pdzk1*$^{-/-}$ mice, weight gain was similar to wild-type mice. Cardiac hypertrophy and fatty liver, both of which are observed in systemic carnitine deficient *jvs* mice with *octn2* gene deficient (Nezu et al., 1999), were not observed in *pdzk1*$^{-/-}$ mice. One of the possible reasons would be a compensatory hyperfunction of amino acid transporters due to the decrease in the oligopeptide transport activity in the small intestine of *pdzk1*$^{-/-}$ mice. It is also possible that metabolism and/or excretion of carnitine might be changed in *pdzk1*$^{-/-}$ mice, thereby carnitine deficiency was not observed. In addition, other adaptor protein(s) than PDZK1 may function as a compensatory regulator of PEPT1 and/or OCTN2 in *pdzk1*$^{-/-}$ mice. Therefore, additional studies are required to clarify the compensatory mechanisms caused by the loss of *pdzk1* gene in the small intestine.

Considering that there is little difference in PEPT1 mRNA level between wild-type and *pdzk1*$^{-/-}$ mice (Fig. 3C), PDZK1 appears to be involved in the post-transcriptional regulation of PEPT1. This might be explained by internalization of PEPT1 in intestinal epithelial cells in *pdzk1*$^{-/-}$ mice. In fact, electron microscopy revealed a remarkable loss of PEPT1 protein in microvilli, whereas immunoreactivity was observed in the cytoplasmic region in intestinal epithelial cells from *pdzk1*$^{-/-}$ mice (Fig. 5B). It is noteworthy that in *pdzk1*$^{-/-}$ mice vesicular structures were more obviously seen in the cytoplasmic region (Fig. 5C, 5D). We have not yet been able to identify these intracellular structures exhibiting immunoreactivity against PEPT1 antibody (Fig. 6B, 6D). Considering the essential role of PDZK1 in the apical localization of PEPT1 *in vivo* (Figs 5, 6), the appearance of such vesicular structures may reflect defective sorting of PEPT1 to apical membranes and/or unstable localization of PEPT1 on the apical membrane surface. Similar loss of PEPT1 expression on the apical membrane was

DMD Fast Forward. Published on March 5, 2008 as DOI: 10.1124/dmd.107.020321
This article has not been copyedited and formatted. The final version may differ from this version.

recently found in small GTP-binding protein *rab8* gene knockout (*rab8*$^{-/-}$) mice (Sato et al., 2007), indicating a pivotal role of Rab8 in sorting of PEPT1 to the apical membranes. However, the regulatory mechanism for PEPT1 is clearly different between Rab8 and PDZK1, since the length of microvilli was reduced in *rab8*$^{-/-}$ mice, and the mutation was lethal just after the weaning period, whereas the reduction in the length of microvilli was not so obvious in *pdzk1*$^{-/-}$ mice, which have normal fertility (Lan and Silver 2005). However, in the present study, we first revealed ultrastructural change in cytoplasm of absorptive epithelial cells in *pdzk1*$^{-/-}$ mice (Fig. 5D).

There has been no report regarding proteins that physically interact with PEPT1; this is the first demonstration of the interaction between PEPT1 and PDZK1 in small intestinal lysates and HEK293 cells transfected with both proteins by immunoprecipitation analysis (Figs. 3A, 2A). This physical interaction between PEPT1 and PDZK1 was unexpected, since, according to our previous yeast two-hybrid analysis, no interaction was observed between the C-terminus of PEPT1 and PDZK1 (Kato et al., 2004), implying that some structural domain(s) other than the C-terminus could be involved in the interaction with PDZK1. This was also confirmed by the present finding that PDZK1 not only stimulated [^{3}H]GlySar uptake by PEPT1, but also that by PEPT1Δ4 (Fig. 1A, 1D). This is in contrast to the regulation by PDZK1 of other SLC transporters (Anzai et al., 2004; Kato et al., 2004, 2005; Miyazaki et al., 2005; Sugiura et al., 2006), in which the PDZ binding motif at the extreme C-terminus is essential for a PDZK1-mediated increase in expression and/or transport activity. Although the PDZ binding motif is localized at the C-terminus of most interacting transporters and receptors, several PDZ domains also recognize a specific internal peptide motif (Hillier et al., 1999). Another possibility would be an indirect interaction of PEPT1 and PDZK1,

via another protein. For example, the small PDZK1-associated protein DD96/MAP17 has been shown to interact directly with PDZK1 as a regulatory mechanism (Pribanic et al., 2003; Silver et al., 2003), but also interacts with the N-terminus of Na^+/Pi-IIa (Pribanic et al., 2003).

In summary, our present findings demonstrate that PDZK1 regulates apical localization of PEPT1 and OCTN2 in the small intestine, and is presumably involved in the gastrointestinal absorption of their substrates *in vivo*. The regulation of PEPT1 localization may be closely related to our recent observation that small GTP-binding protein Rab8 plays pivotal roles in apical localization of PEPT1 *in vivo* (Sato et al., 2007). Thus, PEPT1 does not work alone under physiological conditions, but forms a complex with the other proteins. PDZK1 may also interact with the transporters other than PEPT1 and OCTN2 expressed on apical membranes of small intestine (Wang et al., 2000; Rossman et al., 2005; Kato et al., 2006; Hillesheim et al., 2007), and such protein-protein interactions may also provide functional coupling of these transporters, as proposed in the case of PEPT1 and NHE3 *in vitro* (Watanabe et al., 2005). Therefore, an understanding of protein-protein interactions involving xenobiotic transporters is likely to be important to predict the permeability and gastrointestinal absorption of drugs and drug candidates.

ACKNOWLEDGEMENT

We thank Ms Lica Ishida for technical assistance. We also thank Ms Tomoko Yamada for performing western blot analysis.

REFERENCES

Anzai N, Miyazaki H, Noshiro R, Khamdang S, Chairoungdua A, Shin HJ, Enomoto A, Sakamoto S, Hirata T, Tomita K, Kanai Y, and Endou H (2004) The multivalent PDZ domain-containing protein PDZK1 regulates transport activity of renal urate-anion exchanger URAT1 via its C terminus. *J Biol Chem* **279**: 45942-45950.

Chu XY, Sanchez-Castano GP, Higaki K, Oh DM, Hsu CP, and Amidon GL (2001) Correlation between epithelial cell permeability of cephalexin and expression of intestinal oligopeptide transporter. *J Pharmacol Exp Ther* **299**: 575-582.

Frieman DI and Amidon GL (1990) Passive and carrier-mediated intestinal absorption components of two ACE-inhibitor prodrugs in rats; enalapril and fosinopril. *Pharm Res* **6**: 1043-1047.

Ganapathy V and Leibach FH (1985) Is intestinal peptide transport energized by a proton gradient? *Am J Physiol* **249**: G153-G160.

Gisler SM, Pribanic S, Bacic D, Forrer P, Gantenbein A, Sabourin LA, Tsuji A, Zhao Z, Manser E, Biber J and Murer H (2003) PDZK1. I. A major scaffolder in brush borders of proximal tubular cells. *Kidney Int* **64**: 1733-1745.

Hillesheim J, Riederer B, Tuo B, Chen M, Manns M, Biber J, Yun C, Kocher O, and Seidler U (2007) Down regulation of small intestinal ion transport in PDZK1-(CAP70/NHERF3) deficient mice. *Pflugers Arch* **454**: 575-586.

Hillier BJ, Christopherson KS, Prehoda KE, Bredt DS, and Lim WA (1999) Unexpected modes of PDZ domain scaffolding revealed by structure of nNOS-syntrophin complex. *Science* **284**: 812-815.

Hu M and Amidon GL (1988) Intestinal absorption of captopril in rats. *J Pharm Sci* **77**: 1007-1011.

Kato Y, Yoshida K, Watanabe C, Sai Y, and Tsuji A (2004) Screening of the interaction between xenobiotic transporters and PDZ proteins. *Pharm Res* **21**: 1886-1894.

Kato Y, Sai Y, Yoshida K, Watanabe C, Hirata T, and Tsuji A (2005) PDZK1 directly regulates the function of organic cation/carnitine transporter OCTN2. *Mol Pharmacol* **67**: 734-743.

Kato Y, Sugiura M, Sugiura T, Wakayama T, Kubo Y, Kobayashi D, Sai Y, Tamai I, Iseki S, and Tsuji A (2006) Organic cation/carnitine transporter OCTN2 (Slc22a5) is responsible for carnitine transport across apical membranes of small intestinal epithelial cells in mouse. *Mol Pharmacol* **70**: 1-9.

Kennedy DJ, Leibach FH, Ganapathy V, and Thwaites DT (2002) Optimal absorptive transport of the dipeptide glycylsarcosine is dependent on functional Na^+/H^+ exchange activity. *Pflügers Archiv* **445**: 139-146.

Kocher O, Pal R, Roberts M, Cirovic C, and Gilchrist A (2003) Targeted disruption of the PDZK1 gene by homologous recombination. *Mol Cell Biol* **23**: 1175-1180.

Kramer W, Girbig F, Gutjahr U, Kleemann HW, Leipe I, Urbach H, and Wagner A (1990) Interaction of renin inhibitors with the intestinal uptake system for oligopeptides and ß-lactam antibiotics. *Biochim Biophys Acta* **1027**: 25-30.

Lan D and Silver DL (2005) Fenofibrate induces a novel degradation pathway for scavenger receptor B-I independent of PDZK1. *J Biol Chem* **280**: 23390-23396.

Miyazaki H, Anzai N, Ekaratanawong S, Sakata T, Shin HJ, Jutabha P, Hirata T, He X, Nonoguchi H, Tomita K, Kanai Y, and Endou H (2005) Modulation of renal

apical organic anion transporter 4 function by two PDZ domain-containing proteins. *J Am Soc Nephrol* **16**: 3498-3506.

Nakanishi T, Tamai I, Sai Y, Sasaki T, and Tsuji A (1997) Carrier-mediated transport of oligopeptides in the human fibrosarcoma cell line HT1080. *Cancer Res* **57**: 4118-4122.

Naruhashi K, Sai Y, Tamai I, Suzuki N, and Tsuji A (2002) PepT1 mRNA expression is induced by starvation and its level correlates with absorption transport of cefadroxil longitudinally in the rat intestine. *Pharm Res* **19**: 1417-1423.

Nezu J, Tamai I, Oku A, Ohashi R, Yabuuchi H, Hashimoto N, Nikaido H, Sai Y, Koizumi A, Shoji Y, Takada G, Matsuishi T, Yoshino M, Kato H, Ohura T, Tsujimoto G, Hayakawa J, Shimane M, and Tsuji A (1999) Primary systemic carnitine deficiency is caused by mutations in a gene encoding sodium ion-dependent carnitine transporter. *Nat Genet* **21**: 91-94.

Ohashi R, Tamai I, Nezu J, Nikaido H, Hashimoto N, Oku A, Sai Y, Shimane M, and Tsuji A (2001) Molecular and physiological evidence for multifunctionality of carnitine/organic cation transporter OCTN2. *Mol Pharmacol* **59**: 358-366.

Pribanic S, Gisler SM, Bacic D, Madjdpour C, Hernando N, Sorribas V, Gantenbein A, Biber J, Murer H (2003) Interactions of MAP17 with the NaPi-IIa/PDZK1 protein complex in renal proximal tubular cells. *Am J Physiol* **285**: F784-F791.

Rossmann H, Jacob P, Baisch S, Hassoun R, Meier J, Natour D, Yahya K, Yun C, Biber J, Lackner KJ, Fiehn W, Gregor M, Seidler U, and Lamprecht G (2005) The CFTR associated protein CAP70 interacts with the apical Cl-/HCO3-exchanger DRA in rabbit small intestinal mucosa. *Biochemistry* **44**: 4477-4487.

Sai Y, Tamai I, Sumikawa H, Hayashi K, Nakanishi T, Amano O, Numata M, Iseki S, and Tsuji A (1996) Immunolocalization and pharmacological relevance of oligopeptide transporter PepT1 in intestinal absorption of beta-lactam antibiotics. *FEBS Lett* **392**: 25-29.

Saito H, Ishii T, and Inui K (1993) Expression of human intestinal dipeptide transporter in *Xenopus laevis* oocytes. *Biochem Pharmacology* **45**: 776-779.

Sato T, Mushiake S, Kato Y, Sato K, Sato M, Takeda N, Ozono K, Miki K, Kubo Y, Tsuji A, Harada R, and Harada A (2007) The Rab8 GTPase regulates apical protein localization in intestinal cells. *Nature* **448**: 366-369.

Silver DL, Wang N, Vogel S (2003) Identification of small PDZK1-associated protein, DD96/MAP17, as a regulator of PDZK1 and plasma high density lipoprotein levels. *J Biol Chem* **278**: 28528-28532.

Sugiura T, Kato Y, Kubo Y, and Tsuji A (2006) Mutation in an adaptor protein PDZK1 affects transport activity of organic cation transporter OCTNs and oligopeptide transporter PEPT2. *Drug Metab Pharmacokinet* **21**: 375-383.

Tamai I, Nakanishi T, Hayashi K, Terao T, Sai Y, Shiraga T, Miyamoto K, Takeda E, Higashida H, and Tsuji A (1997) The predominant contribution of oligopeptide transporter PepT1 to intestinal absorption of ß-lactam antibiotics in the rat small intestine. *J Pharm Pharmacol* **49**: 796-801.

Tamai I, Ohashi R, Nezu J, Sai Y, Kobayashi D, Oku A, Shimane M, and Tsuji A (2000) Molecular and functional characterization of organic cation/carnitine transporter family in mice. *J Biol Chem* **275**: 40064-40072.

Thwaites DT, Kennedy DJ, Raldua D, Anderson CMH, Mendoza ME, Bladen CL, and Simmons NL (2002) H^+/dipeptide absorption across the human intestinal

epithelium is controlled indirectly via a functional Na^+/H^+ exchanger. *Gastroenterology* **122**: 1322-1333.

Tsuji A, Nakashima E, Asano T, Nakashima R, and Yamana T (1979) Saturable absorption of amino-cephalosporins by the rat intestine. *J Pharm Pharmacol* **31**: 718-720.

Tsuji A, Nakashima E, Kagami I, and Yamana T (1981) Intestinal absorption mechanism of amphoteric beta-lactam antibiotics I: Comparative antibiotics by in situ rat small intestine. *J Pharm Sci* **70**: 768-772.

Tsuji A, Terasaki T, Tamai I, and Hirooka H (1987) H^+ gradient-dependent and carrier-mediated transport of cefixime, a new cephalosporin antibiotic, across brush-border membrane vesicles from rat small intestine. *J Pharmacol Exp Ther* **241**: 594-601.

Tsuji A and Tamai I (1996) Carrier-mediated intestinal transport of drugs. *Pharm Res* **13**: 963-977.

Wang P, Wang JJ, Xiao Y, Murray JW, Novikoff PM, Angeletti RH, Orr GA, Lan D, Silver DL, and Wolkoff AW (2005) Interaction with PDZK1 is required for expression of organic anion transporting protein 1A1 on the hepatocyte surface. *J Biol Chem* **280**: 30143-30149.

Wang S, Yue H, Derin RB, Guggino WB, and Li M (2000) Accessory protein facilitated CFTR-CFTR interaction, a molecular mechanism to potentiate the chloride channel activity. *Cell* **103**: 169-179.

Wakayama T, Koami H, Yamamoto M, and Iseki S (2004) Expression of the adhesion molecule spermatogenic immunoglobulin superfamily (SgIGSF) in mouse tissues. *Acta Histochem Cytochem* **37**: 365-371.

Watanabe C, Kato Y, Ito S, Kubo Y, Sai Y, and Tsuji A (2005) Na^+/H^+ exchanger 3 affects transport property of H^+/oligopeptide transporter 1. *Drug Metab Pharmacokinet* **20**: 443-451.

Yokogawa K, Higashi Y, Tamai I, Nomura M, Hashimoto N, Nikaido H, Hayakawa J, Miyamoto K, Tsuji A (1999) Decreased tissue distribution of L-carnitine in juvenile visceral steatosis mice. *J Pharmacol Exp Ther* **289**: 224-230.

FOOTNOTES

This study was supported in part by a Grant-in-Aid for Scientific Research provided by the Ministry of Education, Science and Culture of Japan, and a grant from the Mochida Memorial Foundation (Tokyo, Japan) for Medical and Pharmaceutical Research.

DMD Fast Forward. Published on March 5, 2008 as DOI: 10.1124/dmd.107.020321
This article has not been copyedited and formatted. The final version may differ from this version.

FIGURE LEGENDS

Fig. 1 Effect of PDZK1 on uptake of [^{3}H]GlySar or cephalexin by PEPT1 transfected into HEK293 cells.

HEK293/PDZK1 (●) or HEK293 (○) cells were transiently transfected with PEPT1 (A, B, C) or PEPT1Δ4 (D), and uptake of [^{3}H]GlySar (A, B, D) and cephalexin (C) was measured. In panels A, C and D, HEK293/PDZK1 (▲) and HEK293 (△) cells were transiently transfected with pEYFP vector alone as a control experiment. In panel B, uptake of [^{3}H]GlySar at various concentrations was measured for 3 min, and PEPT1-mediated uptake, which was calculated by subtracting the background uptake obtained from vector-transfected cells from the total uptake obtained from PEPT1-transfected cells, in HEK293/PDZK1 (●) or HEK293 (○) cells was analyzed by means of the Eadie-Hofstee plot. The results are shown as mean ± S.E.M. of three determinations. When error bars are not shown, they are smaller than the symbols.

*, Significantly different from the uptake by PEPT1 without PDZK1 ($p < 0.05$).

Fig. 2 Interaction of PEPT1 and PDZK1 heterologously expressed in HEK293 cells.

(A) YFP-PEPT1 or YFP-PEPT1Δ4 was transiently transfected in HEK293/PDZK1 cells, in which myc-tagged PDZK1 is stably expressed. Cell lysate was then prepared, and immunoprecipitation was performed using anti-myc antibody followed by Western blotting with anti-GFP (*left panel*) or anti-myc (*light panel*) antibodies, showing specific co-immunoprecipitation of the two proteins. (*lane 1*; YFP-PEPT1 in HEK293

cells, *lane 2*; YFP in HEK293/PDZK1 cells, *lane 3*; YFP-PEPT1 in HEK293/PDZK1 cells, *lane 4*; YFP-PEPT1Δ4 in HEK293/PDZK1 cells).

(B) HEK293 or HEK293/PDZK1 cells were transiently transfected with YFP-PEPT1, and Western blot analysis was performed for cell lysates using anti-GFP (*upper panel*) or anti-GAPDH antibody as a control (*lower panel*).

(C) YFP-PEPT1 was transiently transfected in HEK293 (*upper*) or HEK293/PDZK1 (*lower*) cells, and the fluorescence of YFP was directly visualized.

Fig. 3 Interaction of PEPT1 with PDZK1 and expression of PEPT1 and OCTN2 in mouse small intestine

(A) Intestinal BBMVs obtained from wild-type mice were immunoprecipitated with anti-PDZK1 antibody or preimmune serum, followed by Western blot analysis using anti-PEPT1 (*upper panel*) or anti-PDZK1 (*lower panel*) antibodies.

(B) Intestinal BBMVs (5 μg protein) from wild-type and *pdzk1*$^{-/-}$ mice were subjected to SDS-polyacrylamide gel electrophoresis followed by Western blot analysis using anti-PEPT1, OCTN2, PDZK1 and ß-actin antibodies.

(C) PEPT1 mRNA levels of small intestine from wild-type (open column) and *pdzk1*$^{-/-}$ mice (closed column) were quantified using a real-time PCR method. Each value is the mean normalized to ß-actin levels.

Fig. 4 Immunohistochemical analysis of PEPT1 expression in the small intestine.

Cryosections of small intestine from wild-type (A, C) and *pdzk1*$^{-/-}$ (B, D) mice were incubated with anti-PEPT1 (A, B) and anti-OCTN2 (C, D) antibodies, and visualized with DAB (arrows). Note: the typical staining pattern of PEPT1 and OCTN2 was

DMD Fast Forward. Published on March 5, 2008 as DOI: 10.1124/dmd.107.020321
This article has not been copyedited and formatted. The final version may differ from this version.

observed in apical membrane of small intestine from wild-type mice, but the intensity of staining was markedly reduced in the epithelial cells of the small intestine from *pdzk1*$^{-/-}$ mice. Magnification, x200.

Fig. 5 Electron microscopic analysis of PEPT1 localization in microvilli of absorptive epithelial cells in wild-type (A, C) and *pdzk1*$^{-/-}$ mice (B, D)

The immunoelectron microscopy revealed that immunoreactivity of PEPT1 was mainly localized in microvilli of absorptive epithelial cells in wild-type mice (A), whereas the weak immunoreactivity of PEPT1 was localized in multi-vesicular bodies (dotted line region) and cytoplasmic vesicles (arrowhead) of absorptive epithelial cells from *pdzk1*$^{-/-}$ mice (B). Transmission electron microscopy of intestinal epithelial cells revealed ultrastructure alteration between wild-type and *pdzk1*$^{-/-}$ mice(C, D). Cytoplasmic vesicular structures were more obvious in some of intestinal absorptive epithelial cells in *pdzk1*$^{-/-}$ mice (D), compared with wild-type mice (C) according to the electron microscopy. Scale bars=500 nm.

Fig. 6 Plasma concentration-time profiles of cephalexin (A), [^{3}H]carnitine (B) and antipyrine (C) after oral administration in wild-type and *pdzk1*$^{-/-}$ mice

Plasma concentration of cephalexin (2 mg/kg), [^{3}H]carnitine (250 ng/kg) and antipyrine (20 mg/kg) was determined in wild-type (○) and *pdzk1*$^{-/-}$ (●) mice after oral administration. Each point represents the mean ± S.E.M. (n = 4-8).

*, Significant difference by Student's t-test ($p < 0.05$).

DMD Fast Forward. Published on March 5, 2008 as DOI: 10.1124/dmd.107.020321
This article has not been copyedited and formatted. The final version may differ from this version.

Fig. 7 Retained amount (%) of [^{3}H]carnitine and [^{14}C]inulin in each segment of the GI tract from wild-type and *pdzk1*$^{-/-}$ mice

[^{3}H]carnitine (A) and [^{14}C]inulin (B) retained in each segment (stomach, upper small intestine, middle small intestine, lower small intestine, cecum, large intestine, total recovery) was measured at 30 min after oral administration in wild-type (open column) and *pdzk1*$^{-/-}$ (closed column). The data are expressed as the mean of at least three experiments.

*, Significant difference by Student's t-test ($p < 0.05$).

Fig. 8 Uptake of [^{3}H]carnitine from the apical surface of small intestine of wild-type and *pdzk1*$^{-/-}$ mice

Small intestines of wild-type and *pdzk1*$^{-/-}$ mice were divided into three parts, and uptake of [^{3}H]carnitine (1.3 nM) by each tissue from wild-type (white column) and *pdzk1*$^{-/-}$ (black columns) was measured for 5 min at 37 ˚C in transport buffer (pH 6.0) by Everted Sac Method. Gray columns represent the uptake of [^{3}H]carnitine in the presence of 20 mM unlabeled carnitine in both strain. Each column represents mean ± S.E.M. of four mice.

*, Significant difference by Student's t-test ($p < 0.05$).

Fig. 1

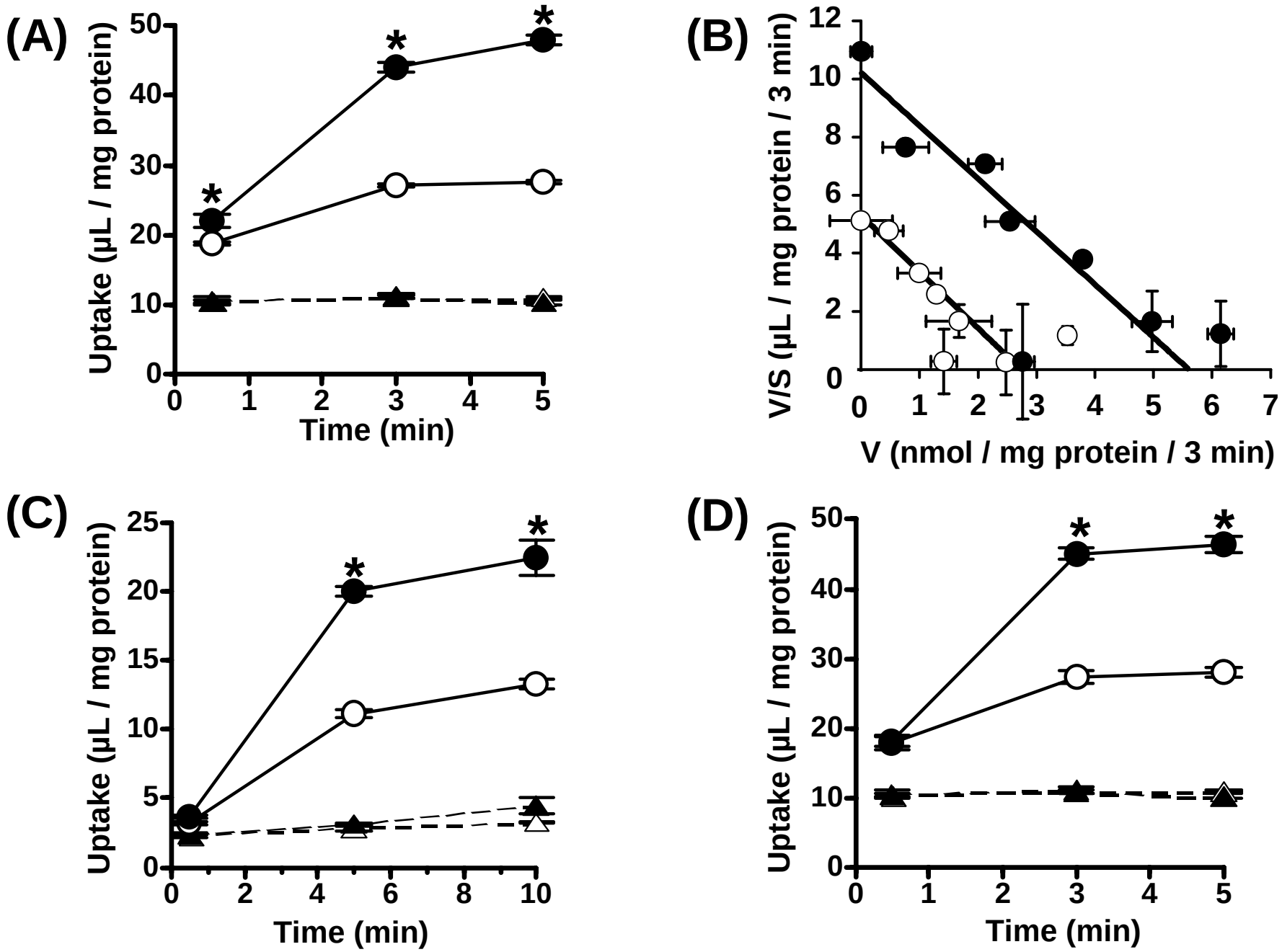

Fig. 2

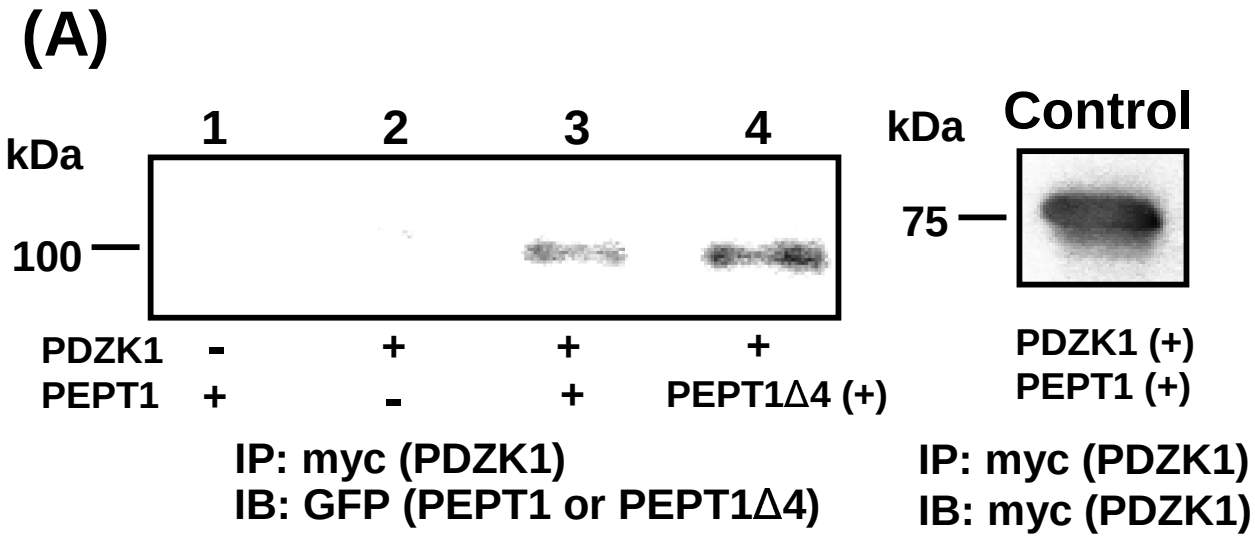

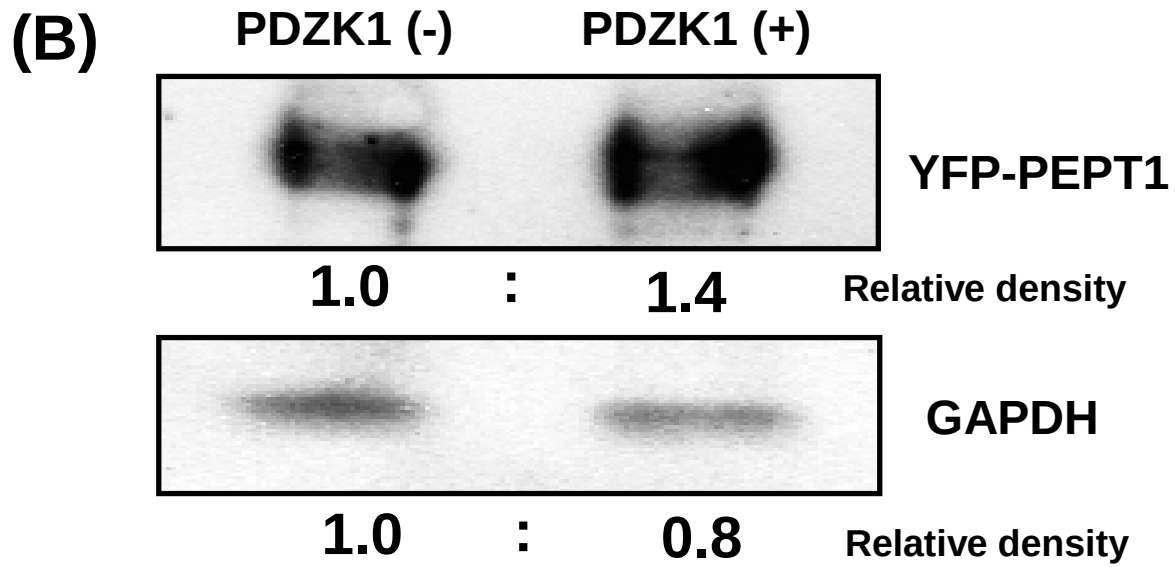

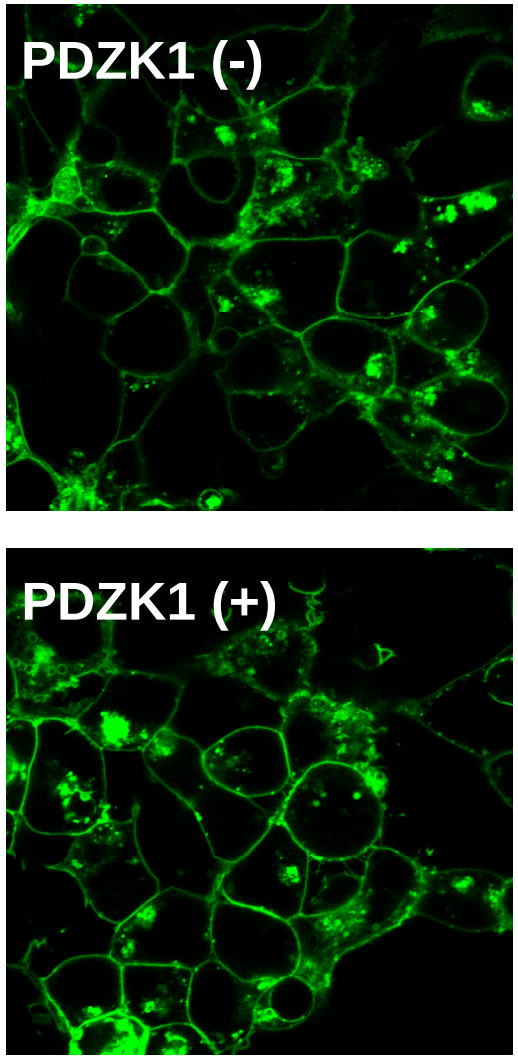

Fig. 3

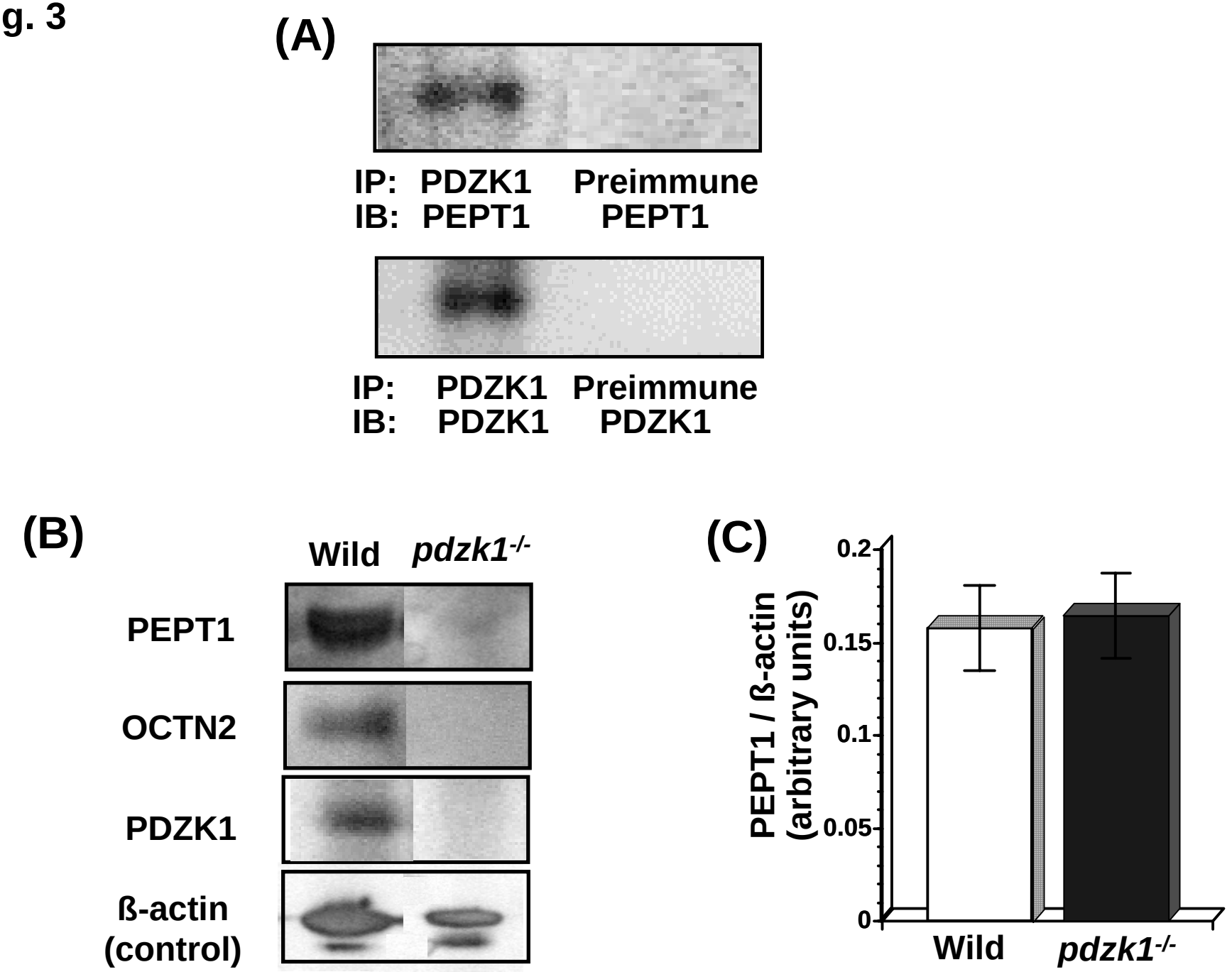

Fig. 4

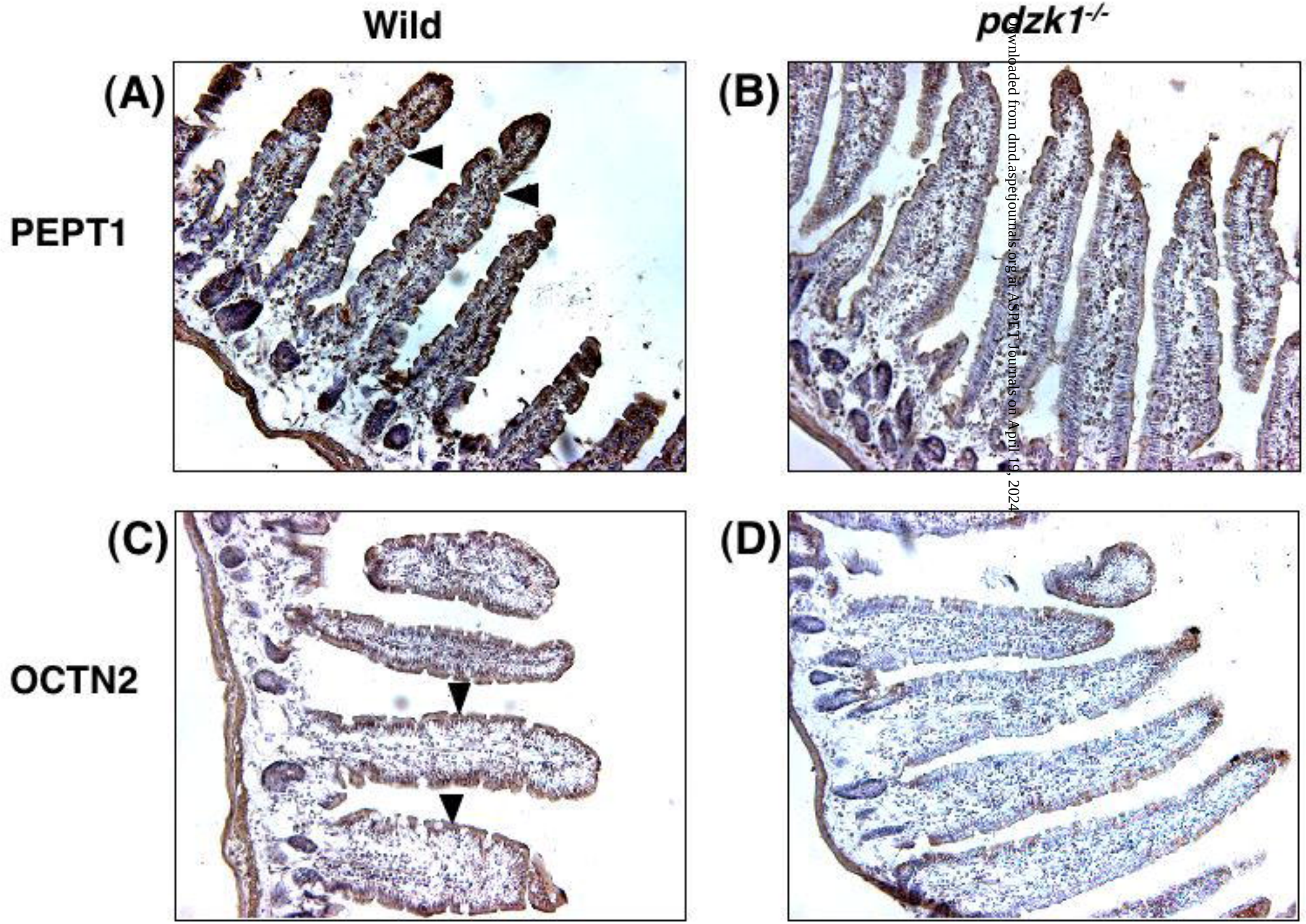

Fig. 5

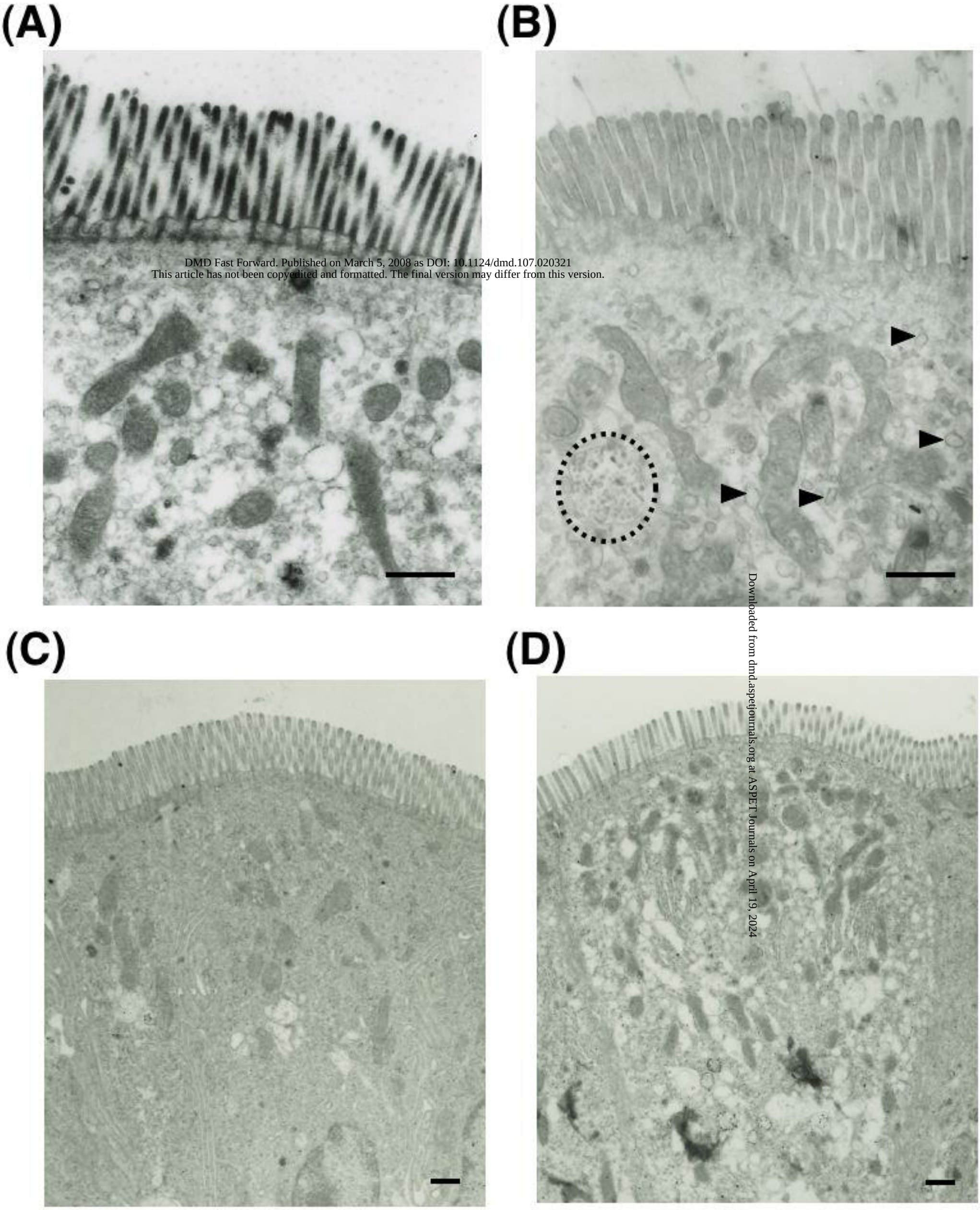

Fig. 6

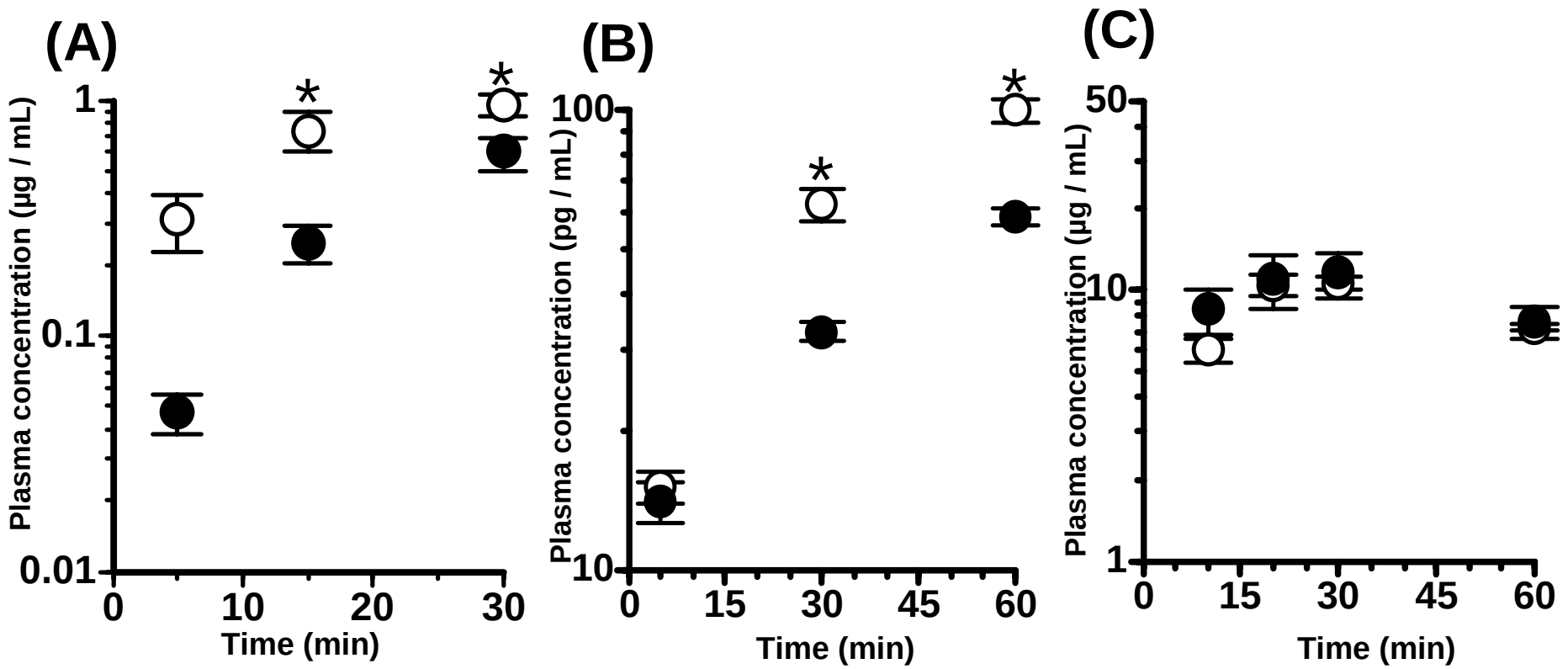

Fig. 7

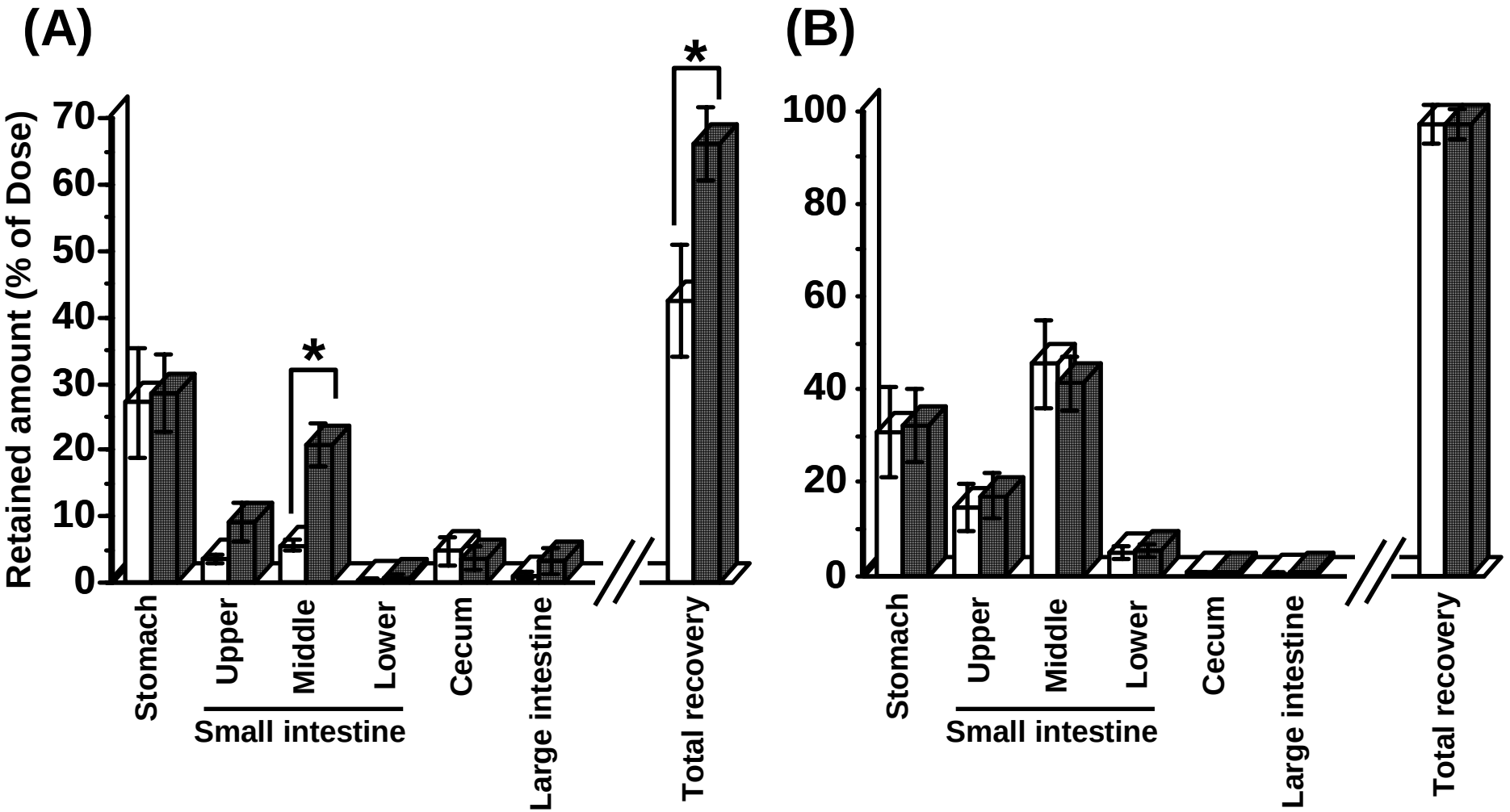

Fig. 8